

Time-lapse Seismic Modeling of CO₂ Sequestration in Geological Formation

S.P. Maurya^{1} and N.P. Singh¹*

Department of Geophysics, Institute of Science, Banaras Hindu University, Varanasi, India- 221005

Email ID: spm.iitb@gmail.com

Keywords: CO₂ Sequestration, Forward Modeling, Gassmann Equations, Seismic Modeling

Summary

Time lapse seismic reservoir modeling can image fluid flow effects in a reservoir if the changes in seismic pattern can be observed. In the present study, Gassmann fluid substitution analysis and forward modeling based on subsurface model has been carried out to predict reservoir response. 2D seismic modeling was performed to simulate the CO₂ injection scenario in the Nisku Formation in the Wabamun area. A decrease in the impedance values are observed in the post-injection scenario and the identification of the CO₂ plume is more evident in the inverted result than in stacked section.

Introduction

The main objective of this study is the seismic modeling and feasibility of monitoring a CO₂ volume after being injected in sandstone aquifers. First, a 2D geological model has been created on the basis of well log information to represent the structure and stratigraphic feature of the subsurface (Kumar and Mohan 2004; Moradi and Lawton 2013). Secondly, the shape and size of CO₂ plume is designed according to the injection volume. The plume is inserted in the targeted formation as second body (Ganguli et al. 2014). This model represents the Post-injection scenario. Subsequently seismic simulation is performed and seismic gathers are generated before and after the CO₂ injection. Next, the time lapse difference are evaluated to demonstrate whether seismic data can be used to monitor the CO₂ plume better or inverted seismic sections in the sandstone target (Herzog 2001).

Finally, the amplitude change was estimated with a time lapse analysis and an inversion study to investigate the capabilities of this technique in detecting is performed the CO₂ plume in the Nisku aquifer.

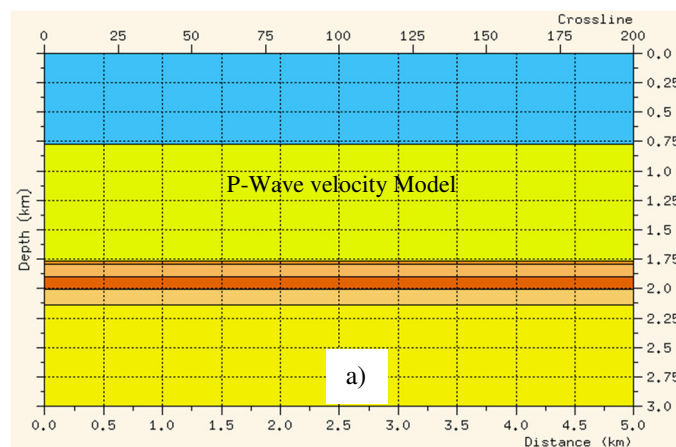
2D Geological Modeling

A 2D geological model was created using Norsar 2D software. To reproduce the structure and stratigraphy of the subsurface gamma ray, velocity and density logs is used. There is no major fault present in the study area (Michael et al., 2008). Seven layers have been identified from top to 3km depth. The depth, velocity and density of all the layers are given in table 1.

Table 1: Geological model parameters. The target formation is indicated in red.

Depth	Vp	Vs	Rho
0.000-0.773	1.910	1.595	2.30
0.773-1.763	3.841	2.091	2.58
1.763-1.793	5.926	3.841	2.74
1.793-1.897	5.500	3.150	2.80
1.897-2.000	6.200	3.300	2.77
2.000-2.140	5.000	2.660	2.80
2.140-3.000	4.000	2.100	2.77

The Model Builder from Norsar software has been used to create this geological model. This option allows defining the geometry of the model. The model is created form horizontal distance of 5km and depth is 3km so dimension is 5kmx3km. A series of interfaces are created within to represents the geological structure of the subsurface on the basis of information given in table 1. The space between the interfaces are called block (Landrø 2002). These blocks are then filled with the geological properties like P-wave velocity (V_p), S-wave velocity (V_s) and Density (ρ). Figure 1 shows baseline geological model. Figure 1a shows geological model filled with P-wave velocity, Figure 1b shows geological model filled with S-wave velocity and Figure 1c shows geological model filled with density. The Nisku formation is fourth layer between depths 1.793km - 1.897km. This depth interval is considered for CO₂ plume simulation.



Time-lapse Seismic Modeling of CO₂ Sequestration

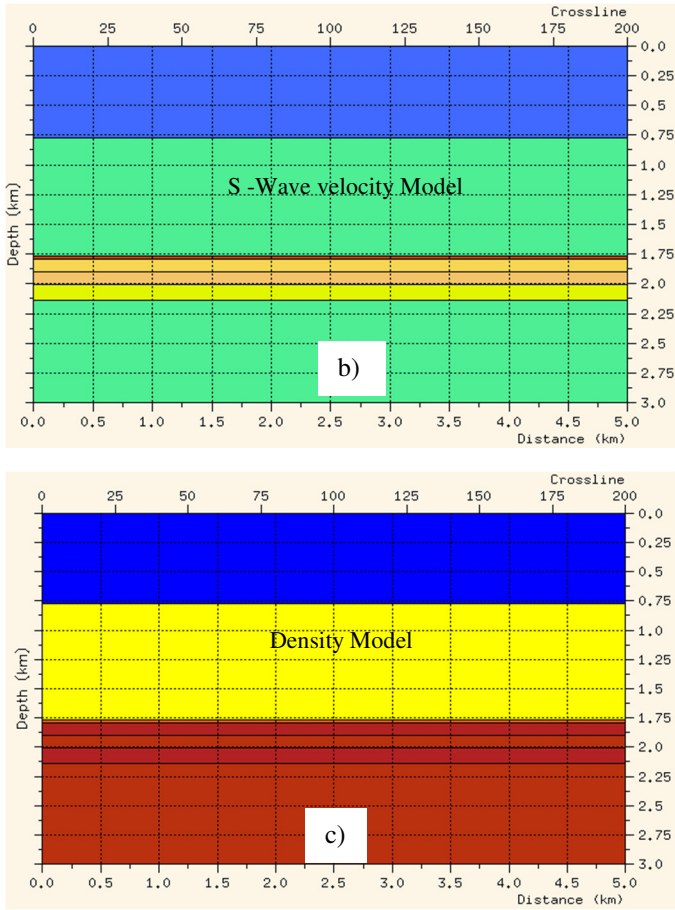


Figure 1: Monitor 2D geological model where a) represents P-wave velocity (V_p), b) represents S-wave velocity (V_s) and c) represents density (ρ) model.

CO₂ Plume Simulation

Frailey (2009) explained the methods for estimating the volume of CO₂ trapped in geological formations. There are two main approaches for this, the first one is static approach and the second one is dynamic. The static approach requires rock and fluid properties while the dynamic approach requires information about active injection, injection volumes and reservoir pressure (Chadwick et al. 2006). The static technique was applied in this study in which a cylinder or disk is selected to estimate the CO₂ volume and corresponding radius of extension (Vera, 2012).

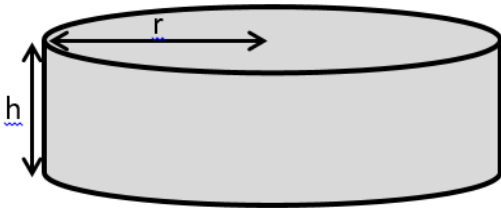


Figure 2: A representative disk model to estimate the CO₂ volume and radius of extension.

The static methods for CO₂ simulation is based on the following equation (White et al. 2003):

$$G_{CO_2} = Ah\varphi E \quad (1)$$

where G_{CO_2} is the CO₂ volume, A is the area, h is the thickness, φ is the porosity, and E is the efficiency which can be equated to average saturation as well. G_{CO_2} is given by

$$G_{CO_2} = \frac{m}{\rho} \quad (2)$$

where m is the mass of CO₂ and ρ is the density under the specific temperature and pressure conditions.

The geometry of the expansion considered in this project is a disk or cylindrical dispersion, having an area of

$$A = \pi r^2 \quad (3)$$

Where r is the radius of the disk for CO₂ expansion. By rearranging the volumetric formula and introducing the precession expansion, r is obtained using the following formula (Sparlin et al. 2010)

$$r = \sqrt{G_{CO_2} / \pi h \varphi E} \quad (4)$$

The simulated amount of CO₂ was 1000000 tons, considered to be the maximum injected mass after 2 years of injection.

Let the thickness be 104m, porosity 7.3% and a CO₂ density under the formation conditions $\rho(CO_2) = 653 \text{ kg/m}^3$. The efficiency would be considered as the saturation of CO₂. The size of the plume was estimated by 100% CO₂ saturation, E = 1.0, using equation 2 (Vera, 2012), the calculated volume is

$$V = \frac{2.0 \times 10^9 \text{ kg}}{653 \text{ kg/m}^3} = 3062787 \text{ m}^3 \quad (5)$$

From the equation, it is possible to calculate now the radius of the disk,

$$r_1 = \sqrt{\frac{V}{h\varphi E\pi}} \Rightarrow \sqrt{\frac{3062787 \text{ m}^3}{104\text{m} * 0.073 * 1.0 * 3.14}} \quad (6)$$

$$\Rightarrow \sqrt{\frac{3062787 \text{ m}^2}{23.84}} = 358.43 \text{ m} \quad (7)$$

Give as a result of approximately 358m. The diameter would be approximately 716m and as previously mentioned, this represents the base and top of the rectangular plume in the 2D model.

The plume is designed in 3D so it looks like cylinder but in this study our focus is 2D modeling so this plume translated to a rectangle in 2D with a longitude equal to the diameter of the cylinder (d=716m) (Mavko et al. 2009). The monitor geological model represents the post-injection scenario. For this case the simulated rectangular CO₂ plume is inserted in

Time-lapse Seismic Modeling of CO₂ Sequestration

the same geological model of the baseline case at Nisku formation (layer 4). Two new interfaces have been created and divided Nisku Formation in three blocks. The left and right blocks have the same properties as for the case of baseline model (representing 0% CO₂ saturation). The third (middle) block represents the injection zone with different velocity and density which are calculated using Gassmann fluid substitution equation (Gassmann, 1951; Smith et al. 2003). The changed velocity and density found from Gassmann equation are shown in table 2.

Table 2: Velocities and density values of the CO₂ plume. The percentages change was obtained from the Gassmann fluid substitution analysis (After Vera 2012).

Properties	% Change	Initial Values	New Values
V _P (m/s)	-4.5	5500	5252.5
V _S (m/s)	0.635	3150	3170
ρ (g/cc)	-1.26	2.8	2.76

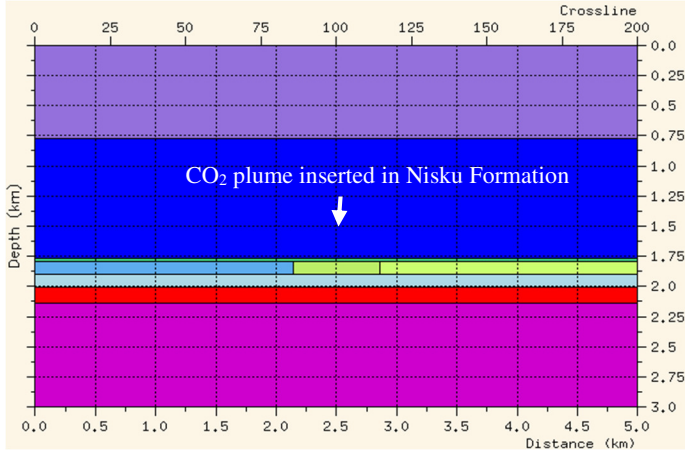


Figure 3: Monitor 2D geological model. The rectangular CO₂ plume is inserted in the Nisku Formation.

2D Seismic Modeling

After successfully generated geological model, 2D seismic survey was designed to generate seismic trace. The purpose to generate seismic section is performing the time lapse analysis for monitoring CO₂ plume (Holloway et al. 2007; Bielinski 2007). The shot and receivers are located every 25m interval, so total number of channel is 200. Next, Norsar 2D 'ray tracing tool' was used to generate reflectivity series which is based on Zoeppritz equations (Vadapalli and Vedanti 2016). After shot simulation, synthetic seismograms are generated using inputs as the seismic events that resulted from the ray tracing and a selected wavelet which is a zero phase ricker wavelet with frequency 40Hz. Figure 4 shows seismic survey design with shots and receiver to generate post stacks seismic gathers.

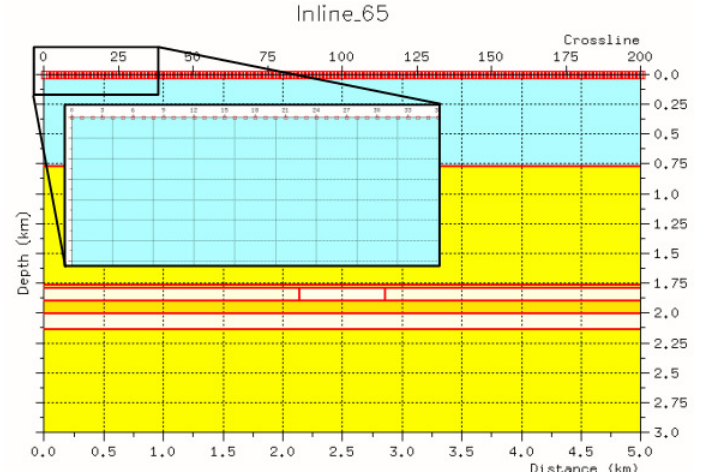


Figure 4: 2D seismic modeling survey design. The line is 5 km long with 25 m shots spacing and 25m receivers spacing.

The seismic section is generated using forward model techniques. From the geological model we have velocity and density from which impedances are calculated using the following equation:

$$Z = V * \rho \quad (8)$$

After getting impedance at all the interfaces, reflectivity of the interface has been calculated using following equation:

$$r_i = \frac{Z_{i+1} - Z_i}{Z_{i+1} + Z_i} \quad (9)$$

where r_i reflectivity of i th is layer and Z_{i+1} is acoustic impedance of $i+1$ th layer and Z_i is acoustic impedance of the i th layer. After getting earth's reflectivity of each layer seismic traces are generated using following equation:

$$S = W * r + n \quad (10)$$

where S is seismic traces, W is wavelet, r is earth's reflectivity and n is noise. Here noise is not included just for simplicity (Maurya and Singh 2017).

2D Seismic Monitoring Results

Once the 2D seismic modeling was completed, the next step was to analyze the changes in physical properties, such as reflectivity, time shift and velocity in the monitor data (Bachu 2000).

Figure 5 shows seismic gathers generated from geological model. The x-axis shows number of traces (200) and y-axis shows time in ms (2000). High amplitude can be seen at each interface. Figure 5a shows seismic gathers for 0% CO₂ case, Figure 5b shows seismic gathers for 100% CO₂ saturation case and Figure 5c shows difference of 5a and 5b and highlighted CO₂ plume zone. To measure changes in acoustic impedance, Model based seismic inversion is performed.

Time-lapse Seismic Modeling of CO₂ Sequestration

Model Based Seismic Inversion

Model based seismic inversion is performed to calculate acoustic impedance contrast from seismic gathers with the help of well log information. The Model Based Inversion (MBI) used the convolutional theory to generate synthetic gathers. The gathers are generated by the convolution of wavelet with the earth's reflectivity with addition of noise (equation 10) (Wang 2001). This technique models the earth's layer in form of acoustic impedance contrast with time. Initially, acoustic impedance model is generated using the interpolation of the impedance logs with the integration of seismic horizons which act as guide to interpolate property (Mallick, 1995; Maurya and Singh, 2015). Basically a low frequency model of the P- impedance are generated and then perturb this model until one obtains a good match between the seismic and computed synthetic seismic trace by using least square optimization techniques (STRATA user guide 2009).

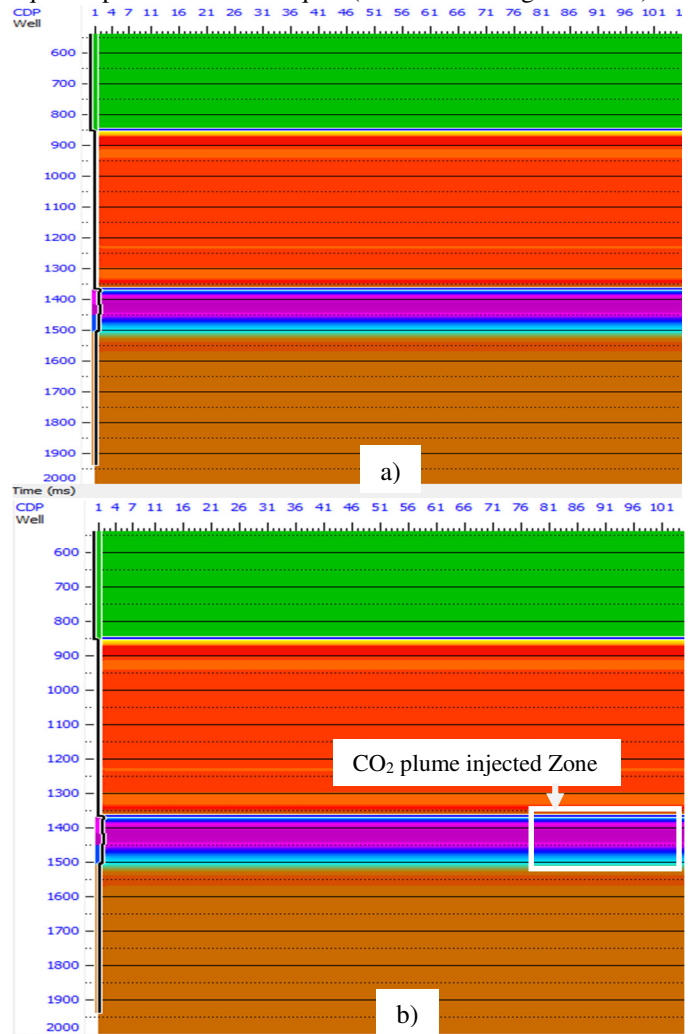


Figure 6: a) Baseline inverted section and b) Monitor inverted section. Distortion in the impedance values in the injection region and reflectors underneath is evident.

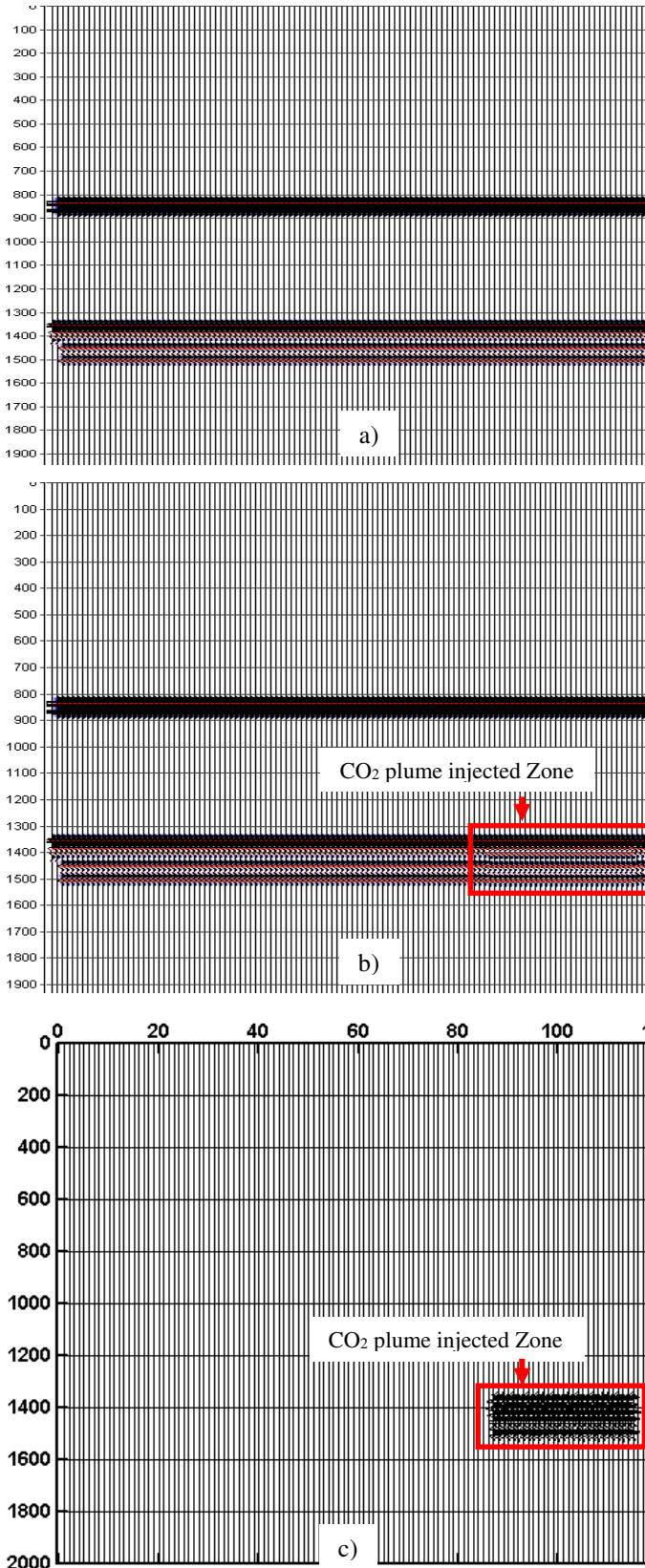


Figure 5: a) Baseline CDP stack section (0% CO₂ saturation), b) Monitor CDP stacked section (100% CO₂ saturation). Injection zone is indicated in black rectangle.

Time-lapse Seismic Modeling of CO₂ Sequestration

Figure 6a shows acoustic impedance contrast for 0% CO₂ scenario. In this sectional the layers are visible more clearly compare to the Amplitude sections. Figure 5b shows acoustic impedance section for 100% CO₂ scenario.

Impedance Comparison after Seismic Inversion:

The changes in the physical properties like velocity, density, reflectivity and time shift caused by the injection of CO₂ in a sandstone aquifer were evaluated using a Gassmann approach (Vera 2012). We attempted to create the geology in the area and simulate the seismic response in order to examine changes produced by CO₂ injection. Figure 5a and 5b shows the monitor CDP stack section compared with the baseline for the 100% CO₂ saturation case. It is possible to see the injection zone and time shift. The effect of CO₂ injection can be determined by subtracting the monitor CDP stack section from the baseline section (0% CO₂).

In addition, a model-based seismic inversion was performed on each CDP stacked section (baseline and monitor) to evaluate the sensitivity of acoustic impedance in detecting the CO₂ plume (Srivastava et al. 2012). Since in this case synthetic data is been used, the first step was to create synthetic well logs (V_P and ρ) to help constrain the impedance initial model. The V_P and density values (Table 1) used to build the 2D geological model are used to create these well logs. The final correlation coefficient was estimated to be 0.95 and 0.96 for baseline and monitor model respectively.

The P-impedance (Z_P) initial model was generated using impedance log calculated with the sonic and density logs from the synthetic well. Since synthetic data is used in this analysis, no low-pass filter was applied in this case. The initial model was generated using the exact impedance values of the synthetic impedance (Z_P) log. Figure 6 shows an example of the inversion analysis performed with the initial model and the baseline CDP stacked section in a window from 0 ms to 2000 ms.

Finally, the model-based seismic inversion was undertaken for both the cases, the baseline and the monitor datasets. Figure 6a shows the inversion results of the baseline CDP stacked (0% CO₂ scenario) section and Figure 6b shows the inversion results of the monitor CDP stacked section (100% CO₂ scenario). The inverted impedance shows the exact impedance values of the initial model except in the monitor case where a distortion is evident in the injection zone and the impedance values of the plume have decreased.

Similar to the differenced stacked sections, Figure 7 shows the effect within the injection zone determined from subtracting the monitor impedance section from the baseline impedance section. This difference represents the 100% CO₂ saturation zone. The traces outside the injection area were cancelled and only the injected region and reflectors below it are affected.

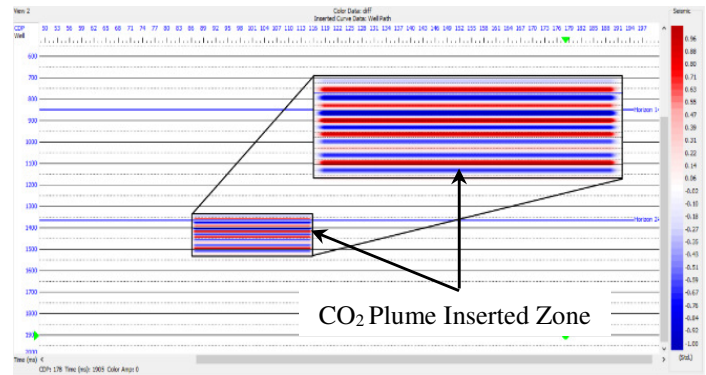


Figure 7: Difference between baseline inversion and monitor inversion. The black rectangle highlights 100% CO₂ injection zone.

It is important to notice that these results identify the shape of the CO₂ plume even more clearly than just by directly comparing the differences in the seismic amplitudes. The top, base and sides of the plume are easily identifiable. The edges of the plume are again located between CDPs 89 and 116. Therefore, the width of the plume is accurately predicted from the inverted section difference (716 m).

Discussion

In this study Seismic modeling is performed to simulate a CO₂ injection in the Nisku saline aquifer. The geological model was created on the basis of seismic and well log information. The shape of the plume is more evident after calculating the difference between the sections where the top and width of the body are clearly distinguishable, while the bottom of the plume is hard to identify due to time delay in deeper reflectors. The 716 m length of the plume was accurately predicted according to the geological model.

Next, to investigate the seismic changes caused by injection of CO₂ a model based seismic inversion has been performed to determine these changes in terms of acoustic impedance contrast. A decrease in the impedance values is observed in the post-injection scenario. As expected, the impedance change is stronger due to the combination of V_P and ρ . In this case, the shape of the plume is even more evident since the base is less affected by the underlying reflectors. It is possible that the impedance changes of the reflectors underneath the plume are not significant and got cancelled after the subtraction process.

The test of inverting the residual CDP stacked section gave interesting results even though the inversion algorithm is designed to use full bandwidth seismic data.

Conclusions

In the CO₂ injection simulation case, the post-injection seismic section shows a time delay of the basal reservoir reflector and amplitude change with respect to the baseline case. Also, a decreased in the impedance values of ~12% is observed in the post-injection scenario. As expected, the impedance change is stronger due to the combination of V_P and ρ . The impedance changes of the reflectors underneath the plume are not

Time-lapse Seismic Modeling of CO₂ Sequestration

significant and got cancelled after subtracting the monitor stacked section from the baseline stacked section and this making the easier identification of the CO₂ plume. The shape of the plume was accurately estimated having a width of 716m.

Acknowledgements

Authers are indebted to Science and engineering Research Board, Department of Science and Technology, New Delhi for financial supports and helps in form of grant no PDF/2016/000888.

References

Bachu, S., 2000, Sequestration of CO₂ in geological media: criteria and approach for site selection in response to climate change. *Energy conversion and Management*, 41 (9), pp.953-970.

Bielinski, A., 2007, Numerical simulation of CO₂ sequestration in geological formations.

Chadwick A., R. Arts., O. Eiken, P. Williamson., and G. Williams., 2006, Geophysical Monitoring of the CO₂ Plume at Sleipner, North Sea: *Advances in the Geological Storage of Carbon Dioxide*, 303-314.

Frailey, S.M., 2009, Methods for estimating CO₂ storage in saline reservoirs. *Energy Procedia*, 1(1), pp. 2769-2776.

Ganguli, S. S., Vedanti, N., Akervoll, I., and Bergmo, P., 2014, An estimation of CO₂-EOR Potential from a sector model in a mature oil field, cambay Basin, India. In Annual convention, IGU-Kurukshethra.

Gassmann, F., 1951, Elastic waves through a packing of spheres. *Geophysics*, 16(4), pp. 673-685.

Herzog, H.J., 2001, Peer reviewed: what future for carbon capture and sequestration?.

Holloway, S., Garg, A., Kapshe, M., Pracha, A.S., Khan, S.R., Mahmood, M.A., Singh, T. N., Kirk K.L., Applequist, L.R., Deshpande, A., Evans, D.J., Garg, Y., Vincent, C.J., and Williams, J.D.O., 2007, A regional assessment of the potential for CO₂ storage in the Indian subcontinent, Sustainable and Renewable Energy Programme Commissioned Report CR/07/198 by British Geological Survey (BGS). Sustainable and Renewable Energy Programme Commissioned Report CR/07/198, British Geological Survey (BGS), NERC.

Kumar, A., and Mohan, S., 2004, Feasibility Assessment of a Time-Lapse Seismic Survey for Thermal EOR in Balol Field, India, Based on Rock Physics and Seismic Forward Modeling. In Proceedings of the 5th International Conference and Exposition on Petroleum Geophysics, Society of Petroleum Geophysicists, pp: 688-695.

Landrø, M., 2002, Uncertainties in quantitative time-lapse seismic analysis. *Geophysical Prospecting*, v.50, no.5, pp: 527-538.

Maurya, S. P. and Singh, K. H. 2017, Bandlimited Impedance Inversion of Blackfoot field, Alberta, Canada. *Journal of Geophysics*, 38 (1), pp.57-61.

Maurya, S.P. and Singh, K.H. 2015, June. LP and ML Sparse Spike Inversion for Reservoir Characterization-A Case Study from Blackfoot Area, Alberta, Canada. In 77th EAGE Conference and Exhibition 2015.

Mavko, G., Mukerji, T., and Dvorkin, J., 2009, *The rock physics handbook: Tools for seismic analysis of porous media*. Cambridge university press.

Michael, K., Bachu, S., Buschkuehle, B., Haug, K., & Talman, S., 2008, Comprehensive Characterization of a Potential Site for CO₂ Geological Storage in Central Alberta, Canada: American Association of Petroleum Geologists Manuscript, 40.

Moradi, S., and Lawton, D. C., 2013, Theoretical detectability of CO₂ at a CCS project in Alberta: 83rd Ann. Internat. Mtg., Soc Expl. Geophys. Expanded Abstract, pp: 3475-3479.

Smith, T. M., Sondergeld, C. H., and Rai, C. S., 2003, Gassmann fluid substitutions: A tutorial. *Geophysics*, v.68, no.2, pp: 430-440.

Sparlin, M., Meyer, J., Bevc, D., Cabrera, R., Hibbitts, T., and Rogers, J., 2010, Seismic analysis and characterization of a brine reservoir for CO₂ sequestration: 80th Ann. Internat. Mtg: Soc. of Expl. Geophys, pp:2304-2308.

Srivastava, R. P., Vedanti, N., Dimri, V. P., Akervol, I., Bergmo, P., and Biram, R. S., 2012, November. CO₂-EOR: A Feasibility Study of an Indian Oil Field. In SEG Annual Meeting. Society of Exploration Geophysicists.

STRATA user guide., 2009, Hampson-Russell Assistant: STRATA Theory. Hampson-Russell Software, a CGG Company.

Vadapalli V. and Vedanti N., 2016, Time-lapse seismic response evaluation based on well log data for Ankleshwar reservoir, Cambay basin, India *J. Ind. Geophys. Union* v.20, no.5, pp: 472-481

Vera, V. C., 2012, CO₂ Seismic modelling of CO₂ in a sandstone aquifer, Priddis, Alberta: M.Sc. Thesis, Univ. of Calgary.

Wang, Z., 2001. Fundamentals of seismic rock physics. *Geophysics*, v.66, no.2, pp: 398-412.

White, C.M., Strazisar, B.R., Granite, E.J., Hoffman, J.S. and Pennline, H.W., 2003, Separation and capture of CO₂ from large stationary sources and sequestration in geological formations—coalbeds and deep saline aquifers. *Journal of the Air & Waste Management Association*, 53(6), pp.645-715.